Published in final edited form as:
Proteomics. 2009 February ; 9(3): 768–782. doi:10.1002/pmic.200800385.

Mass spectrometric and computational analysis of cytokine-induced alterations in the astrocyte secretome

Sarah Dunn Keene[1,*], **Todd M. Greco**[1,*], **Ioannis Parastatidis**[1], **Seon-Hwa Lee**[2], **Ethan G. Hughes**[3], **Rita J. Balice-Gordon**[3], **David W. Speicher**[4], and **Harry Ischiropoulos**[1,2]

1 *Stokes Research Institute and Department of Pediatrics, Children's Hospital of Philadelphia, Philadelphia, PA, USA*

2 *Department of Pharmacology, University of Pennsylvania School of Medicine, Philadelphia, PA, USA*

3 *Department of Neuroscience, University of Pennsylvania School of Medicine, Philadelphia, PA, USA*

4 *The Wistar Institute, Philadelphia, PA, USA*

Abstract

The roles of astrocytes in the CNS have been expanding beyond the long held view of providing passive, supportive functions. Recent evidence has identified roles in neuronal development, extracellular matrix maintenance, and response to inflammatory challenges. Therefore, insights into astrocyte secretion are critically important for understanding physiological responses and pathological mechanisms in CNS diseases. Primary astrocyte cultures were treated with inflammatory cytokines for either a short (1 day) or sustained (7 days) exposure. Increased interleukin-6 secretion, nitric oxide production, cyclooxygenase-2 activation, and nerve growth factor (NGF) secretion confirmed the astrocytic response to cytokine treatment. MS/MS analysis, computational prediction algorithms, and functional classification were used to compare the astrocyte protein secretome from control and cytokine-exposed cultures. In total, 169 secreted proteins were identified, including both classically and nonconventionally secreted proteins that comprised components of the extracellular matrix and enzymes involved in processing of glycoproteins and glycosaminoglycans. Twelve proteins were detected exclusively in the secretome from cytokine-treated astrocytes, including matrix metalloproteinase-3 (MMP-3) and members of the chemokine ligand family. This compilation of secreted proteins provides a framework for identifying factors that influence the biochemical environment of the nervous system, regulate development, construct extracellular matrices, and coordinate the nervous system response to inflammation.

Keywords

Astrocytes; Comparative proteomics; Cytokines; Development; Protein secretion

1 Introduction

Appreciation for the function of astrocytes in the CNS has been growing with the identification of integral roles in neurogenesis and synaptogenesis [1,2]. Specifically, astrocytic secretion of

Correspondence: Dr. Harry Ischiropoulos, Stokes Research Institute, Children's Hospital of Philadelphia, 416D Abramson Research Center, 3517 Civic Center Boulevard, Philadelphia, PA 19104-4318, USA, E-mail: ischirop@mail.med.upenn.edu, Fax: +1-215-590-4267.
*These authors contributed equally to this work.

The authors have declared no conflict of interest.

glutamate, ATP, and D-serine serve as paracrine and autocrine factors regulating synaptic plasticity and the coordination of synaptic networks [3,4]. Astrocytes are also important components of the blood brain barrier, providing dynamic regulation of the microvasculature through the release of nitric oxide and lipid metabolites [5,6], as well as modulating brain energy metabolism through the coordination of glutamate homeostasis between neurons and astrocytes [7,8].

In contrast, the release of proteins by astrocytes under nondisease states has not been extensively explored. Proteins released by astrocytes include thrombospondin-1 and apolipoprotein E, which were found to mediate synaptogenesis and processing of amyloid-β peptides, respectively [9,10]. The advent of MS-based proteomics has allowed for the global interrogation of astrocyte proteomes, including intra-cellularly expressed proteins as well as secreted proteins [11–14]. However, only a limited number of proteins have been detected in the astrocyte secretome. Therefore, an expanded proteome of astrocyte-secreted proteins employing recent advances in proteomic methodology, instrumentation, and computational analyses is warranted. A more comprehensive astrocyte secretome would provide new insights into astrocyte function and uncover novel mediators that can influence the extracellular biochemical environment in the CNS.

Astrocytes play a critical role in regulating the type and extent of CNS immune response by responding to inflammatory mediators such as interferon (IFN)-γ and TNF-α and by producing additional cytokines and chemokines [15]. While an inflammatory response is necessary following tissue and cellular injury, it is also seen as a central process in the development and progression of disease states. Under certain pathological conditions, recent studies provide evidence that astrocytes secrete factors that are toxic to other cells in the CNS. For example, in patients with multiple sclerosis, astrocytes expressing syncytin released factors that are toxic to oligodendrocytes [16]. Recently, soluble factors released from astrocytes that expressed familial amyotrophic lateral sclerosis (ALS)-causing mutant forms of superoxide dismutase 1-induced motor neuron death [17–20]. Collectively, these data emphasize that astrocytes under pathological conditions are capable of unleashing toxic, but in many cases unidentified factors. Insights into the factors secreted by astrocytes after treatment with inflammatory mediators may identify disease mediators and reveal targets for the therapy.

2 Materials and methods

2.1 Astrocyte culture and cytokine treatment

All mouse studies were reviewed and approved by the Institutional Animal Care and Use Committee of the Stokes Research Institute, Children's Hospital of Philadelphia. Cortical astrocyte cultures were prepared from neonatal CD-1 mice (Charles River, Wilmington, MA) on DOL 1–2. Briefly, the animals were anesthetized, the brain was removed and cortex was dissected free. Cortices were washed twice with Earle's Balanced Salt Solution (EBSS; Invitrogen, Carlsbad, CA) and trypsinized (0.05%) for 12 min at 37°C. Cortices were then titruated in Minimal Essential Media (Invitrogen, Carlsbad, CA) supplemented with 10% FBS (Hyclone), sodium pyruvate (1 mM), L-glutamine (2 mM), D-glucose (42 mM), sodium bicarbonate (14 mM), penicillin (100 U/mL), streptomycin (100 μg/mL), fungizone (2.5 μg/mL) and plated at one cortex *per* T-25 vent-cap flask (Corning, Corning, NY). Mixed cortical cultures were raised for 14 days in 37°C and 5% CO_2 with media change every 3–4 days. Cultures were then washed with cold EBSS and separated from neurons and microglia by shaking overnight at 37°C. Adherent cells were trypsinized (0.25%) and seeded in 100 mm Petri dishes (Corning) at 5×10^6 cells/plate (6 mL). Forty-eight hours after plating, cells were washed with EBSS, and serum-free media was added containing IL-1β (0.2 ng/mL), IFN-γ (1 ng/mL), and TNF-α (10 ng/mL) (Roche Pharmaceuticals, Switzerland). Control astrocytes were cultured in serum-free media alone. Astrocyte-conditioned media (ACM) was either

collected after 24 h (1D ACM) or were either left untreated or treated with the cytokine cocktail (see above) every 48 h for an additional 6 days (three total exposures) with no media change. ACM was again collected (7 days ACM). For each collection, ACM was combined from two plates and centrifuged at 200×g for 5 min to remove cell debris. The protein fraction (>3 kDa) was obtained by ultra-filtration of ACM using CentriPrep Ultracel YM-3 filters (Millipore, Billerica, MA). The protein retentate (final vol. = 0.8–1.0 mL) was aliquoted and stored at −80° C for future use. Filtrates were reserved for lipid analyses. To assess cell viability, astrocytes were trypsinized and combined with cell pellets obtained from the low speed centrifugation of ACM. Cell death was quantified either by flow cytometry using Vybrant Apoptosis Assay Kit #3 according to the manufacturer's instructions (Invitrogen, Carlsbad, CA) or by trypan blue exclusion. For flow cytometry, a minimum of 20 000 events was required for each analysis performed in quadruplicate.

2.2 Gel/LC-MS/MS analysis of conditioned media

The protein fraction obtained from ACM was analyzed by Gel/LC-MS/MS as described previously [21]. For each treatment condition described above, the concentrated protein fraction was mixed with 6X Laemmli sample buffer and equal volumes (30 μL) were loaded on NuPAGE 10% Bis-Tris gels (Invitrogen, Carlsbad, CA) and electrophoresed in MOPS running buffer for approximately 2 cm. For experiments that assessed reproducibility, ACM was collected and proteins were separated by electrophoresis from independent astrocyte cultures (biological duplicates) treated for 7 days with and without cytokines. Proteins were visualized by Colloidal Blue (Invitrogen, Carlsbad, CA) and each lane was cut into uniform slices using a MEF-1.5 Gel Cutter (The Gel Company, San Francisco, CA). Gel slices were digested in-gel with trypsin as previously described [22]. Tryptic digests were analyzed on an LTQ linear IT mass spectrometer (Thermo Electron, San Jose, CA) coupled with a NanoLC pump (Eksigent Technologies, Livermore, CA) and auto-sampler. Tryptic peptides were separated by RP-HPLC on a nanocapillary column, 75 μm id × 20 cm PicoFrit (New Objective, Woburn, MA, USA), packed with MAGIC C_{18} resin, 5 μm particle size (Michrom BioResources, Auburn, CA). Solvent A was 0.58% acetic acid in Milli-Q water, and solvent B was 0.58% acetic acid in ACN. Peptides were eluted into the mass spectrometer at 200 nL/min using an ACN gradient. Each RP-LC run consisted of a 10 min sample load at 1% B; a 75 min total gradient consisting of 1–28% B over 50 min, 28–50% B over 14 min, 50–80% B over 5 min, 80% B for 5 min before returning to 1% B in 1 min. To minimize carryover, a 36 min blank cycle was run between each sample. Hence, the total sample-to-sample cycle time was 121 min. The mass spectrometer was set to repetitively scan *m*/*z* from 375 to 1600 followed by data-dependent MS/MS scans on the ten most abundant ions with dynamic exclusion enabled.

2.3 Protein identification and validation

DTA files were generated from MS/MS spectra extracted from the RAW data file (intensity threshold of 5 000; minimum ion count of 30) and processed by the ZSA, CorrectIon, and IonQuest algorithms of the SEQUEST Browser program. Database searching was performed by TurboSE-QUEST v.27 (rev. 14) against the NCBI nonredundant protein database (4 379 558 proteins; 1/2007), which had been indexed with the following parameters: average mass range of 500–3500, length of 6–100, tryptic cleavages with one internal missed cleavage sites, static modification of Cys by carboxyamidomethylation (+57 amu), and variable modification of methionine (+16 amu). The DTA files were searched with a 2.5 amu peptide mass tolerance and 1.0 amu fragment ion mass tolerance. Potential sequence-to-spectrum peptide assignments generated by SEQUEST were loaded into Scaffold (version Scaffold-01_06_17, Proteome Software, Portland, OR) to validate MS/MS peptide and protein identifications as well as to compare protein identifications across experimental conditions. Peptide and protein probabilities were calculated by the Peptide and Protein Prophet algorithms [23,24],

respectively. A protein was identified if it received ≥99.0% protein confidence with ≥3 unique peptides at ≥95% confidence. A protein that received ≥99.0% protein confidence with two peptides at ≥50% probability was considered identified only if the same protein had been identified by the above criteria in another treatment group. If either of these criteria were not satisfied, the protein was considered to be low confidence and was scored as not detected. Proteins identifications not assigned to the *Mus musculus* taxonomy were manually inspected. These proteins were either contaminants and were removed in the final analysis, or contained identified peptides identical to the mouse sequence and therefore, based on rules of parsimony, were considered to be of mouse origin.

2.4 Computational and functional gene ontology analysis

NCBI database protein identifiers (gi) were matched to equivalent entries (accession) in the Uniprot database (www.uniprot.org), and if known, were reported as unprocessed precursors. Protein Prowler (http://pprowler.imb.uq.edu.au/) was used to identify proteins that possess a secretory pathway (SP) signal peptide (SP score>mTP/Other). Cytoscape/BiNGO was used to perform gene ontology (GO) assignments and determine significantly under-and over-represented functional GO categories. Cytoscape network visualization platform (ver 2.5; 7/23/2007; http://www.cytoscape.org/) implementing the latest release of the BiNGO plugin (ver 2.0; 1/17/2007;http://www.psb.ugent.be/cbd/papers/BiNGO/) [25] was used to identify proteins that were annotated to the extracellular space (GO: 5 576) and cell surface (GO: 9 986). Analyses were performed using the default BiNGO mouse annotation containing 19 224 members (1/12/2007; ftp://ftp.ncbi.nlm.nih.gov/gene/DATA/) and either the GOSlim_GOA or GO_Full ontology (12/18/2006; http://www.geneontology.org). Statistical significance was determined by hypergeomtric analysis followed by Benjamini and Hochberg false discovery rate (FDR) correction ($p<0.001$). SecretomeP 2.0 (http://www.cbs.dtu.dk/services/SecretomeP/) was used to evaluate proteins that may be nonclassically secreted ($p>0.5$) in conjunction with prior experimental evidence. The proteins designated as secretory/extracellular were assigned to broad functional categories relevant to extracellular functions. SledgeHMMER [26] was used to perform batch searching of the Pfam database, followed by conversion of Pfam entries to their equivalent InterPro domain (release 14.1; http://www.ebi.ac.uk/inter-pro/).

3 Results

3.1 Cytokine-induced responses of murine astrocytes

Enriched neonatal cortical astrocyte cultures were prepared as described in the Materials and Methods and were treated under serum-free conditions with either vehicle (control) or TNF-α (10 ng/mL), interleukin (IL)-1β (0.2 ng/mL), and IFN-γ (1 ng/mL) for either an acute (1 day) or sustained (7 days) exposure interval. Cell viability evaluated by flow cytometry after 1 day or 7 days did not significantly differ between control and cytokine-exposed cells (Fig. 1B of Supporting Information). Astrocyte activation by inflammatory mediators induced stereotypical morphological changes such as process formation and elongation (Fig. 1A of Supporting Information). These changes were quantified by counting the number of cells with processes, which revealed that 1 day and 7 days cytokine treatment significantly increased the percent of cells with processes compared to untreated cultures (Fig. 1A). In addition, the percent of cells with processes was also significantly increased from 1 day to 7 days of cytokine treatment (Fig. 1A).

Astrocytic responses to cytokine treatment were further characterized for each exposure interval by quantifying well-characterized markers of inflammation, namely IL-6, nitric oxide, and prostaglandin E_2 (PGE_2) in ACM (See Materials and Methods of Supporting Information). After 1 day and 7 days treatment with inflammatory mediators, robust production of IL-6 was

detected in ACM compared to the control conditions (Fig. 1B). The concentration of nitric oxide metabolites measured by reductive chemistries coupled to chemiluminescence detection was significantly increased in ACM compared to controls following 1 day and 7 days inflammatory mediator treatment (Fig. 1C). Astrocytic responses to inflammatory mediators are also characterized by increased production of prostaglandins, such as prostaglandin E_2 (PGE_2), which is the most abundant prostanoid in the CNS. A lipidomic profile of 24 lipids was carried out on ACM using LC-electron capture atmospheric pressure chemical ionization/multiple reaction monitoring (APCI/MRM) MS analysis. Absolute quantification was performed against standard curves constructed using authentic lipids and normalized to deuterated lipid internal standards (Fig. 1D). These analyses revealed a selective increase of PGE_2 (retention time (rt) = 31.0 min) after 7 days cytokine treatment (0.49 ± 0.03 pmol/10^6 cells to 1.50 ± 0.12 pmol/10^6 cells; Fig. 1D). In contrast, there was no difference in the levels of $PGF_{2\alpha}$ (rt = 33.0 min) detected in ACM from control (0.12 ± 0.01 pmol/10^6 cells) and cytokine-treated (0.13 ± 0.01 pmol/10^6 cells) astrocytes (Fig. 1D).

While controlled inflammation is critical for innate immune defense as well as cellular remodeling and tissue repair, unregulated inflammation would clearly be detrimental. Therefore, glia, one of the primary immune cells in the CNS, possesses compensatory, anti-inflammatory mechanisms to limit the scope of inflammation. In particular, trophic factors such as nerve growth factor (NGF) have been identified as initiators of signaling cascades that promote anti-inflammatory processes following proinflammatory events [27]. Consistent with this mechanism, we detected significantly elevated levels of NGF only after 7 days cytokine treatment compared to 7 days control (203.2 ± 158.4 pg/mL *vs*. 964.2 ± 433.7 pg/mL; $P = 0.0025$). Collectively, morphological evaluation, flow cytometry analysis, and quantification of IL-6, nitric oxide, and lipid markers of inflammatory responses established the secretory capacity, viability, and stereotypical responses to inflammatory mediators.

3.2 Proteomic evaluation of the astrocyte secretome

Extracellular and secretory proteins play a fundamental role in transforming the extracellular space and facilitating cell–cell contacts, such as during development or after synaptic remodeling following brain injury [28]. While neuron–neuron communication has been an area of intense study during synaptogenesis, the capacity of astrocytes to influence this process, specifically through secreted proteins, is not completely understood. Toward this goal, we employed a proteomic approach to identify soluble proteins secreted by murine astrocytes under control and cytokine-treated conditions. The protein fraction of ACM from control or cytokine-treated cultures was obtained by ultrafiltration and was subjected to Gel/LC-MS/MS analysis. Briefly, proteins were separated by 1-D PAGE for approximately 2 cm and visualized by Colloidal blue (Fig. 2A of Supporting Information). Each lane was cut into 12 equal slices and digested in-gel with trypsin [22]. Tryptic digests were then analyzed by nanocapillary RP-LC interfaced directly with a linear IT mass spectrometer (Thermo LTQ) operated in data dependent mode [21]. MS/MS sequence-to-spectrum assignments were generated using the SEQUEST algorithm searching against the NCBI nr database. SEQUEST search results from the 12 LC-MS/MS runs that comprised a complete proteome, *i.e*, a complete gel lane, were combined into a single biological sample within Scaffold (Proteome Software, Portland, OR). Scaffold served as a validation tool, employing the PeptideProphet and ProteinProphet algorithms, which provide statistical evaluation of the SEQUEST results by expressing potential sequence-to-spectrum assignments as confidence scores [23,24]. A protein was identified if it received ≥99.0% protein confidence with ≥3 unique peptides at ≥95% confidence. A protein that received ≥99.0% protein confidence with two peptides at ≥50% probability was considered identified only if the same protein had been identified by the criteria listed above in another treatment group. If either of these criteria were not satisfied, the protein

was considered to be low confidence and was scored as not detected. In total, 290 proteins were identified across all treatment groups (Table 1, and Table 1 of Supporting Information).

The ability to compare and contrast protein identifications across several conditions is highly dependent upon the reproducibility of the treatment conditions and the proteomic approach. Gel/LC-MS/MS analysis of 7 days ACM biological duplicates from control and cytokine-treated conditions showed 96% protein identity. As an additional measure of technical reproducibility, frequency *versus* fold difference in spectral counts (redundant peptides) between biological duplicates for each confirmed protein was calculated (Fig. 2B of Supporting Information). Both 7 days control and cytokine-treated conditions showed similar reproducibility, with >85% of the confirmed proteins varying by ≤2.5 fold between biological duplicates. Importantly, slicing and analyzing the entire gel lane enabled identification of substantially more proteins than single protein band excision while not compromising depth of analysis or reproducibility as 90% of the proteins identified by a single band excision were confirmed by the Gel/LC-MS/MS method (data not shown). The high reproducibility of the experimental design and proteomic method paired with rigorous selection criteria permitted us to compare and contrast proteins identified between control and cytokine-treated conditions.

3.3 Computational and functional classification of secretory proteins

Previous studies have investigated mouse astrocyte intracellular proteomes [13,14], but only two studies have explored the secreteome, identifying a total of 40 unique proteins by 2-D SDS-PAGE and MALDI-TOF-MS [11,12]. The current study found 38 of these proteins while identifying an additional 252. Since previous studies identified primarily the most abundant proteins contained within the secreteome, a rigorous analysis to distinguish between secreted/extra-cellular proteins and other nonsecreted/intracellular proteins, which may be present due to cell death, was not necessary. In the current study, cell death was unchanged (~15%) and cytokine-independent across all treatment conditions as quantified by flow cytometry (Fig. 1 of Supporting Information) and trypan blue exclusion (data not shown). Yet, given the increased sensitivity of the current approach it was critical that the potential contribution of differences in depth of analysis be considered.

We addressed these potential differences in depth of analysis by evaluating the protein identifications using a multi-step computational workflow. For the human proteome, cellular localization for only about 30% of all proteins has been determined experimentally [29], making *in silico* localization prediction algorithms valuable computational tools for the analysis of secreted proteomes [30]. Since the majority of soluble proteins destined for secretion into the extracellular space contain an N-terminal signal peptide, many computational algorithms utilize this feature for sub-cellular localization prediction. The use of trained neural networks and support vector machines has improved the overall performance of these algorithms. In particular, we utilized Protein Prowler [31] for its excellent specificity (0.99) and sensitivity (0.91; Nonmembrane) [30]. Protein Prowler analysis predicted 149 proteins to contain an N-terminal signal peptide (Table 2 of Supporting Information). Yet recent studies have clearly documented that not all extracellular/secreted proteins adhere to the N-terminal rule [32]. To maximize inclusion of secreted proteins that may lack an N-terminal signal, we utilized two complementary approaches. First, GO analysis was performed using Cytoscape network visualization software implementing the BiNGO plug-in. An additional 14 proteins were classified that lacked an identifiable signal peptide, but had been annotated to the extra-cellular region (GO: 5 576) or the cell surface (GO: 9 986). Second, a sequence-based prediction algorithm for non-classical secretion, SecretomeP [33], was employed in conjunction with existing experimental evidence. An additional six proteins that likely proceed *via* nonclassical secretion were included as a result of this analysis, including vimentin, an intermediate filament

protein secreted by activated macrophages [34], as well as annexin A2 [35] and cyclophilin A [36].

Given that the majority of secreted proteins become enriched in conditioned media between 1 day and 7 days compared to nonsecreted proteins, the average fold change in relative protein abundance for proteins classified as secreted should be significantly greater than the changes in relative protein abundance of nonsecreted proteins, which are largely identified due to uniform cell death (Fig. 1 of Supporting Information). To test this hypothesis, semi-quantitative MS based on label-free spectral counting was employed. This method has been previously used as an effective means to estimate relative protein abundance [37–42]. While semi-quantitative MS based on spectral counting can be used to compare the relative abundance between different proteins, for example by normalizing spectral counts by either the protein molecular weight or by the number of observable tryptic peptides, our goal was to compare relative changes of the same protein across experimental conditions. Therefore, we simply compared the number of redundant peptides, *i.e*., spectral counts, for each protein between experimental conditions (Tables 3 and 4 of Supporting Information). Supporting this hypothesis, the average, absolute fold change of spectral counts from 1 day to 7 days was significantly different ($P<0.0001$) for the proteins classified in the secretome (3.9 ± 0.4, mean ± SEM, $N = 79$) (Table 3 of Supporting Information) than for the proteins that were assigned as "nonsecretory" (2.1 ± 0.1, mean ± SEM, $N = 84$) (Table 4 of Supporting Information).

While post-hoc analyses cannot achieve complete sensitivity for the classification of secretory proteins, by utilizing multiple complementary analyses, namely *in silico* cellular localization prediction algorithms, functional GO classification, and published experimental evidence, we generated a list of 169 high confidence secretory proteins, which could be assigned to seven broad functional categories (Fig. 2A). The list included expected extracellular matrix proteins, such as laminins and collagens, proteins involved in processing and proteolysis, such as matrix metalloproteinase-3 (MMP-3) and cathepsins, as well as proteins that play critical roles in the immune response, such as the complement components and chemokine ligands. A complete list of these proteins and their corresponding numbers of unique peptides are reported in Table 1. InterPro domain analysis of these proteins was consistent with the InterPro domains of 2 033 proteins that were computationally predicted to be soluble, secreted proteins from the mouse genome [43]. Significantly, the EGF-like domain (IPR000561) was the most common domain in both the theoretical [43] and experimental mouse secretomes (Fig. 2B). To ascertain specific molecular and biological processes that were represented among the proteins identified in the astrocyte secretome (Table 1), we used GO classification to assign proteins into molecular, biological, and cellular subcategories, followed by functional network analysis using hypergeometric statistics paired with multiple testing correction ($p<0.001$) (see Materials and Methods). As shown in Fig. 2C, proteins with molecular functions assigned to protein binding ($P = 2.6E-5$) as well as enzyme regulator ($P = 1.5E-7$), hydrolase ($P = 4.9E-7$), isomerase ($P = 6.4E-7$), and oxidoreductase ($P = 1.8E-4$) activities were over-represented. The biological process ontology contained proteins significantly over-represented in development ($P = 4.1E-8$) and response to stimulus ($P = 2.6E-5$). The proteins that remained unclassified (Table 1 of Supporting Information) were significantly over-represented in catabolism ($P = 1.5E-26$) and macromolecule metabolism ($P = 3.3E-5$) (data not shown), further supporting the computational and functional analysis workflow was largely successful in classifying extracellular and secretory proteins.

3.4 Basal and cytokine-induced alterations in the astrocyte secretome

The effects of proinflammatory cytokines on the astrocyte secretome (Table 1) were compared after 1 day and 7 days of conditioning. Under control conditions, 80 proteins were identified from 1 day ACM, which subsequently increased to 109 upon cytokine stimulation (Fig. 3A).

In contrast, the total and unique numbers of proteins identified in 7 days ACM between control and cytokine conditions were more similar (Fig. 3B). The relative decrease in unique proteins at 7 days *versus* 1 day post cytokine treatment can be partially attributed to the substantial basal protein secretion, as evidenced by the 77 proteins that were unique to 7 days control *versus* 1 day control (Fig. 3C) and by the related increase in total secreted protein in 7 days ACM as visualized by SDS–PAGE (Fig. 2A of Supporting Information). Yet this did not preclude identification of proteins which were unique to 1 day or 7 days conditions. Overall, 15 proteins were exclusively detected in control ACM ("d" in Table 1), while 12 proteins were exclusively detected in ACM only after cytokine treatment ("c" in Table 1). These cytokine-specific proteins included MMP-3 and four members of the chemokine ligand family, consistent with their central roles in immune response. Interestingly, three of the chemokine ligands, chemokine (C–C motif) ligand 7, chemokine (C–C motif) ligand 8, and chemokine (C–X3–C motif) ligand 1, were detected only after 7 days cytokine treatment, while chemokine, (C–X–C motif) ligand 1 was also identified under the 1 day exposure condition.

To reveal potential functional alterations in the population of secretory proteins resulting from 7 days cytokine, changes in relative protein abundance were examined with respect to functional category. In this analysis, a protein was considered increased relative to control if it (i) was exclusively detected in 7 days cytokine samples or (ii) had a ≥2.5-fold increase in relative protein abundance (RPA) as assessed by the number of redundant peptides (spectral counts) (Table 3 of Supporting Information). A protein was considered significantly decreased relative to control if it (i) was exclusively detected in 7 days control samples or (ii) had a ≥2.5-fold decrease in RPA (Table 3 of Supporting Information). RPA changes were calculated for the shared protein IDs between 7 days control and 7 days cytokine conditions (Fig. 3B, circle overlap). Using these criteria, a total of 36 proteins (13 proteins unique to 7 days cytokine ACM plus 23 proteins with increased RPA) identified after 7 days cytokine treatment were considered significantly increased relative to 7 days control. Of these, 28 and 33% were associated with immune response and extracellular matrix and adhesion, respectively (Fig. 4A). In contrast, 40 proteins (19 proteins unique to 7 days control ACM plus 21 proteins with decreased RPA) were considered significantly decreased after 7 days cytokine stimulation. Interestingly, compared to the group of protein with increased RPA, proteins with decreased RPA comprised a smaller portion of immune response (8%) and extracellular matrix and adhesion (15%), whereas those associated with metabolism (23%) were now the most prominent (Fig. 4B). Notably, there were no significant decreases in RPA under control conditions from 1 day to 7 days suggesting that the observed decreases in RPA of metabolic enzymes after 7 days cytokine treatment was due to the cytokine exposure and not to a decreased secretion over time. A similar analysis was not performed at the 1 day time point, as there were too few proteins with significant decreases in RPA to perform functional comparisons.

Western blot analysis was performed for several of the proteins identified in the astrocyte secretome to (i) confirm their identification by MS and (ii) corroborate the spectral counting analysis. Consistent with the increase in spectral counts, complement C3 and ceruloplasmin show an increase upon cytokine treatment, while the cytokine-induced decrease in ApoE protein levels support the observed decrease in spectral counts (Fig. 5A). Importantly, chemokine ligand 1, which was exclusively identified by MS under cytokine-treated conditions (Table 1), was also only detected by Western analysis under these conditions (Fig. 5B).

4 Discussion

The astrocyte secretome represents a relatively unexplored proteome but one with increasing interest and importance as astrocytes play vital roles in CNS development and synaptic communication. While activated astrocytes are a hallmark of many CNS pathologies, and as

such their responses to inflammatory mediators have been studied extensively [44], a broad characterization of astrocyte-secreted biomolecules had not been performed. Here, we report a systematic secretome analysis from murine astrocytes under control and cytokine-treated conditions, which mimicked both acute (1 day) and more sustained (7 days) exposure to inflammatory mediators. Using validated proteomic approaches coupled with stringent selection criteria and a multistep bioinformatic workflow, 169 extracellular/secreted proteins were identified from ACM. This study confirmed a majority of known astrocyte-secreted proteins [9–12], while identifying more than 100 proteins not previously ascribed to astrocyte protein secretion. Proteins identified in the secretome included components of the extracellular matrix and proteins involved in extracellular protein processing and metabolism, which are consistent with known functions of astrocytes in the maintenance and restructuring of the extracellular scaffolding. The secretome also included members of the insulin-like growth factor binding proteins and cystatin C, known to provide growth support for stem cells, neurons and astrocytes. In addition, we identified many lesser-known or studied components of the astrocyte ECM such as nidogen-2, cathepsins, proteinase inhibitors, and glucosamine transferases, which may not only regulate the composition of the ECM, but also serve as signaling molecules in a paracrine or autocrine fashion. Interestingly, one of the largest functional categories containing protein with decreased RPA was metabolism (Fig. 4B). This included several enzymes, such as hexosaminidase B and β-glucuronidase, involved in protein glycosylation as well as the processing of glycosaminoglycans (GAGs). Deficiencies in these classes of proteins are associated with various lysosomal storage diseases, such as Sandhoff's disease and the mucopolysaccharidosis disorders, which can exhibit a diversity of CNS deficits [45,46].

The study also found secretion of four ligands from the C–C, C–X–C, and C–X3–C chemokine ligand families upon cytokine stimulation. These low molecular weight proteins have diverse biological function in the CNS, including the regulation of inflammation [47,48] and the migration of oligondendrocyte precursors [49] and neural stem cells [50]. The C–X–C ligand 1, which was the only chemokine identified 1 day after inflammatory stimulation, is expressed in reactive astrocytes in mice models of multiple sclerosis [51] and although not toxic to oligodendrocytes may prevent their migration into demyelinated regions. The secretion of these chemokines may also have autocrine functions resulting in the elaboration of other inflammatory mediators such as products of the cyclooxygenase pathway and nitric oxide synthases. Quantitative lipidomics determined that PGE_2, and $PGF_{2\alpha}$ but not other lipid mediators of arachidonic acid metabolism were selectively secreted by astrocytes, and that only PGE_2 is significantly elevated upon cytokine treatment. Interestingly, elevated levels of PGE_2 have been documented in the cerebrospinal fluid (CSF) of patients with neurodegenerative diseases [52].

While the majority of classically secreted proteins are produced as unprocessed precursors that contain signal sequences, directing them through the traditional ER/Golgi secretion pathway, a limited number of proteins have been identified that do not contain signal sequences, but yet are still actively secreted [32]. Of the 169 proteins reported in the astrocyte secretome, 12% did not contain an N-terminal signal sequence. Many of these proteins have been documented as proceeding through nonclassical secretory pathways including macrophage inhibitory factor (MIF), galectin-3, phosphatidylethanolamine-binding protein 1 (PEBP-1), vimentin, meteorin, and acyl CoA-binding protein (ACBP) [32,34,53–55]. Interestingly, the secretion of ACBP, also known as diazepam binding inhibitor (DBI), was originally described as a glial derived factor [54], and recent findings suggest that its secretion may require the Golgi-associated protein GRASP secretory pathway [56]. Another protein of potential interest, meteorin, has been previously identified as a developmentally secreted protein that facilitates astrocyte formation and glial cell differentiation and can support neuron axonal extension [57].

Global proteomic analyses of conditioned cellular media resulted in the identification of secreted and extra-cellular proteins as well as nonsecreted proteins, which in part can be ascribed to cellular death. Given the depth of analysis afforded by current proteomic approaches, computational means are necessary for rapid, unbiased evaluation of protein secretomes. The current approach provides a computational workflow that can be applied in a systematic fashion to analyze protein identifications from any biological secretome. Importantly, the identification of secreted proteins with distinct export mechanisms highlights the utility of this model system for elucidating the molecular mechanisms that govern the regulation and functionality of protein secretion. Overall, this systematic proteomic analysis provides a comprehensive profile of the astrocyte secretome that can be used as a reference for evaluating the impact of individual or multiple components on CNS physiology.

Supplementary Material

Refer to Web version on PubMed Central for supplementary material.

Acknowledgements

The authors would like to thank Dr. Ian Blair for his assistance and expertise in lipidomic profiling and Kaye Speicher for her helpful discussions on the proteomic analysis. The work was supported by grants from the National Institutes of Health NIA AG13966 and ES013508 NIEHS Center of Excellence in Environmental Toxicology. HI is the Gisela and Dennis Alter Research Professor of Pediatric Neonatology at the Children's Hospital of Philadelphia.

Abbreviations

ACM
: astrocyte-conditioned media

ALS
: amyotrophic lateral sclerosis

APCI/MRM/MS
: atmospheric pressure chemical ionization/multiple reaction monitoring/MS, CNS

GO
: gene ontology

IFN
: interferon

MMP-3
: matrix metalloproteinase-3

NGF
: nerve growth factor

References

1. Garcia AD, Doan NB, Imura T, Bush TG, Sofroniew MV. GFAP-expressing progenitors are the principal source of constitutive neurogenesis in adult mouse forebrain. Nat Neurosci 2004;7:1233–1241. [PubMed: 15494728]
2. Mauch DH, Nagler K, Schumacher S, Goritz C, et al. CNS synaptogenesis promoted by glia-derived cholesterol. Science 2001;294:1354–1357. [PubMed: 11701931]
3. Pascual O, Casper KB, Kubera C, Zhang J, et al. Astrocytic purinergic signaling coordinates synaptic networks. Science 2005;310:113–116. [PubMed: 16210541]

4. Volterra A, Meldolesi J. Astrocytes from brain glue to communication elements: the revolution continues. Nat Rev Neurosci 2005;6:626–640. [PubMed: 16025096]
5. Mulligan SJ, MacVicar BA. Calcium transients in astrocyte endfeet cause cerebrovascular constrictions. Nature 2004;431:195–199. [PubMed: 15356633]
6. Zonta M, Angulo MC, Gobbo S, Rosengarten B, et al. Neuron-to-astrocyte signaling is central to the dynamic control of brain microcirculation. Nat Neurosci 2003;6:43–50. [PubMed: 12469126]
7. Bernardinelli Y, Magistretti PJ, Chatton JY. Astrocytes generate Na+-mediated metabolic waves. Proc Natl Acad Sci USA 2004;101:14937–14942. [PubMed: 15466714]
8. Escartin C, Valette J, Lebon V, Bonvento G. Neuron-astrocyte interactions in the regulation of brain energy metabolism: a focus on NMR spectroscopy. J Neurochem 2006;99:393–401. [PubMed: 17029594]
9. Christopherson KS, Ullian EM, Stokes CC, Mullowney CE, et al. Thrombospondins are astrocyte-secreted proteins that promote CNS synaptogenesis. Cell 2005;120:421–433. [PubMed: 15707899]
10. Koistinaho M, Lin S, Wu X, Esterman M, et al. Apolipo-protein E promotes astrocyte colocalization and degradation of deposited amyloid-beta peptides. Nat Med 2004;10:719–726. [PubMed: 15195085]
11. Delcourt N, Jouin P, Poncet J, Demey E, et al. Difference in mass analysis using labeled lysines (DIMAL-K): a new, efficient proteomic quantification method applied to the analysis of astrocytic secretomes. Mol Cell Proteomics 2005;4:1085–1094. [PubMed: 15905179]
12. Lafon-Cazal M, Adjali O, Galeotti N, Poncet J, et al. Proteomic analysis of astrocytic secretion in the mouse. Comparison with the cerebrospinal fluid proteome. J Biol Chem 2003;278:24438–24448. [PubMed: 12709418]
13. Egnaczyk GF, Pomonis JD, Schmidt JA, Rogers SD, et al. Proteomic analysis of the reactive phenotype of astrocytes following endothelin-1 exposure. Proteomics 2003;3:689–698. [PubMed: 12748948]
14. Yang JW, Rodrigo R, Felipo V, Lubec G. Proteome analysis of primary neurons and astrocytes from rat cerebellum. J Proteome Res 2005;4:768–788. [PubMed: 15952724]
15. Dong Y, Benveniste EN. Immune function of astrocytes. Glia 2001;36:180–190. [PubMed: 11596126]
16. Antony JM, van Marle G, Opii W, Butterfield DA, et al. Human endogenous retrovirus glycoprotein-mediated induction of redox reactants causes oligodendrocyte death and demyelination. Nat Neurosci 2004;7:1088–1095. [PubMed: 15452578]
17. Cassina P, Pehar M, Vargas MR, Castellanos R, et al. Astrocyte activation by fibroblast growth factor-1 and motor neuron apoptosis: implications for amyotrophic lateral sclerosis. J Neurochem 2005;93:38–46. [PubMed: 15773903]
18. Di Giorgio FP, Carrasco MA, Siao MC, Maniatis T, Eggan K. Noncell autonomous effect of glia on motor neurons in an embryonic stem cell-based ALS model. Nat Neurosci 2007;10:608–614. [PubMed: 17435754]
19. Nagai M, Re DB, Nagata T, Chalazonitis A, et al. Astrocytes expressing ALS-linked mutated SOD1 release factors selectively toxic to motor neurons. Nat Neurosci 2007;10:615–622. [PubMed: 17435755]
20. Vargas MR, Pehar M, Cassina P, Martinez-Palma L, et al. Fibroblast growth factor-1 induces heme oxygenase-1 via nuclear factor erythroid 2-related factor 2 (Nrf2) in spinal cord astrocytes: consequences for motor neuron survival. J Biol Chem 2005;280:25571–25579. [PubMed: 15870071]
21. Tang HY, Ali-Khan N, Echan LA, Levenkova N, et al. A novel four-dimensional strategy combining protein and peptide separation methods enables detection of low-abundance proteins in human plasma and serum proteomes. Proteomics 2005;5:3329–3342. [PubMed: 16052622]
22. Speicher K, Kolbas O, Harper S, Speicher D. Systematic analysis of peptide recoveries from in-gel digestions for protein identifications in proteome studies. J Biomol Tech 2000;11:74–86.
23. Keller A, Nesvizhskii AI, Kolker E, Aebersold R. Empirical statistical model to estimate the accuracy of peptide identifications made by MS/MS and database search. Anal Chem 2002;74:5383–5392. [PubMed: 12403597]
24. Nesvizhskii AI, Keller A, Kolker E, Aebersold R. A statistical model for identifying proteins by MS/MS. Anal Chem 2003;75:4646–4658. [PubMed: 14632076]

25. Maere S, Heymans K, Kuiper M. BiNGO: a Cytoscape plugin to assess overrepresentation of gene ontology categories in biological networks. Bioinformatics 2005;21:3448–3449. [PubMed: 15972284]
26. Chukkapalli G, Guda C, Subramaniam S. SledgeHM-MER: a web server for batch searching the Pfam database. Nucleic Acids Res 2004;32:W542–W544. [PubMed: 15215445]
27. Villoslada P, Genain CP. Role of nerve growth factor and other trophic factors in brain inflammation. Prog Brain Res 2004;146:403–414. [PubMed: 14699976]
28. Lukes A, Mun-Bryce S, Lukes M, Rosenberg GA. Extracellular matrix degradation by metalloproteinases and central nervous system diseases. Mol Neurobiol 1999;19:267–284. [PubMed: 10495107]
29. Nair R, Rost B. Mimicking cellular sorting improves prediction of subcellular localization. J Mol Biol 2005;348:85–100. [PubMed: 15808855]
30. Klee EW, Sosa CP. Computational classification of classically secreted proteins. Drug Discov Today 2007;12:234–240. [PubMed: 17331888]
31. Hawkins J, Boden M. Detecting and sorting targeting peptides with neural networks and support vector machines. J Bioinform Comput Biol 2006;4:1–18. [PubMed: 16568539]
32. Nickel W. Unconventional secretory routes: direct protein export across the plasma membrane of mammalian cells. Traffic 2005;6:607–614. [PubMed: 15998317]
33. Bendtsen JD, Jensen LJ, Blom N, Von Heijne G, Brunak S. Feature-based prediction of nonclassical and leaderless protein secretion. Protein Eng Des Sel 2004;17:349–356. [PubMed: 15115854]
34. Mor-Vaknin N, Punturieri A, Sitwala K, Markovitz DM. Vimentin is secreted by activated macrophages. Nat Cell Biol 2003;5:59–63. [PubMed: 12483219]
35. Zhao WQ, Chen GH, Chen H, Pascale A, et al. Secretion of Annexin II via activation of insulin receptor and insulin-like growth factor receptor. J Biol Chem 2003;278:4205–4215. [PubMed: 12431980]
36. Suzuki J, Jin ZG, Meoli DF, Matoba T, Berk BC. Cyclophilin A is secreted by a vesicular pathway in vascular smooth muscle cells. Circ Res 2006;98:811–817. [PubMed: 16527992]
37. Liu H, Sadygov RG, Yates JR III. A model for random sampling and estimation of relative protein abundance in shotgun proteomics. Anal Chem 2004;76:4193–4201. [PubMed: 15253663]
38. Old WM, Meyer-Arendt K, Aveline-Wolf L, Pierce KG, et al. Comparison of label-free methods for quantifying human proteins by shotgun proteomics. Mol Cell Proteomics 2005;4:1487–1502. [PubMed: 15979981]
39. Rappsilber J, Ryder U, Lamond AI, Mann M. Large-scale proteomic analysis of the human spliceosome. Genome Res 2002;12:1231–1245. [PubMed: 12176931]
40. Schmidt MW, Houseman A, Ivanov AR, Wolf DA. Comparative proteomic and transcriptomic profiling of the fission yeast *Schizosaccharomyces pombe*. Mol Syst Biol 2007;3:79. [PubMed: 17299416]
41. Liu Q, Tan G, Levenkova N, Li T, et al. The proteome of the mouse photoreceptor sensory cilium Complex. Mol Cell Proteomics 2007;6:1299–1317. [PubMed: 17494944]
42. Ishihama Y, Oda Y, Tabata T, Sato T, et al. Exponentially modified protein abundance index (emPAI) for estimation of absolute protein amount in proteomics by the number of sequenced peptides per protein. Mol Cell Proteomics 2005;4:1265–1272. [PubMed: 15958392]
43. Grimmond SM, Miranda KC, Yuan Z, Davis MJ, et al. The mouse secretome: functional classification of the proteins secreted into the extracellular environment. Genome Res 2003;13:1350–1359. [PubMed: 12819133]
44. Pekny M, Nilsson M. Astrocyte activation and reactive gliosis. Glia 2005;50:427–434. [PubMed: 15846805]
45. Donsante A, Levy B, Vogler C, Sands MS. Clinical response to persistent, low-level beta-glucuronidase expression in the murine model of mucopolysaccharidosis type VII. J Inherit Metab Dis 2007;30:227–238. [PubMed: 17308887]
46. Denny CA, Alroy J, Pawlyk BS, Sandberg MA, et al. Neurochemical, morphological, and neurophysiological abnormalities in retinas of Sandhoff and GM1 gangliosidosis mice. J Neurochem 2007;101:1294–1302. [PubMed: 17442056]

47. Bezzi P, Domercq M, Brambilla L, Galli R, et al. CXCR4-activated astrocyte glutamate release via TNFalpha: amplification by microglia triggers neurotoxicity. Nat Neurosci 2001;4:702–710. [PubMed: 11426226]
48. Babcock AA, Kuziel WA, Rivest S, Owens T. Chemokine expression by glial cells directs leukocytes to sites of axonal injury in the CNS. J Neurosci 2003;23:7922–7930. [PubMed: 12944523]
49. Tsai HH, Frost E, To V, Robinson S, et al. The chemokine receptor CXCR2 controls positioning of oligodendrocyte precursors in developing spinal cord by arresting their migration. Cell 2002;110:373–383. [PubMed: 12176324]
50. Imitola J, Raddassi K, Park KI, Mueller FJ, et al. Directed migration of neural stem cells to sites of CNS injury by the stromal cell-derived factor 1alpha/CXC chemokine receptor 4 pathway. Proc Natl Acad Sci USA 2004;101:18117–18122. [PubMed: 15608062]
51. Glabinski AR, Tani M, Strieter RM, Tuohy VK, Ransohoff RM. Synchronous synthesis of alpha- and beta-chemokines by cells of diverse lineage in the central nervous system of mice with relapses of chronic experimental auto-immune encephalomyelitis. Am J Pathol 1997;150:617–630. [PubMed: 9033275]
52. Combrinck M, Williams J, De Berardinis MA, Warden D. Levels of CSF prostaglandin E2, cognitive decline, and survival in Alzheimer's disease. J Neurol Neurosurg Psychiatry 2006;77:85–88. [PubMed: 15944180]
53. Flieger O, Engling A, Bucala R, Lue H, et al. Regulated secretion of macrophage migration inhibitory factor is mediated by a nonclassical pathway involving an ABC transporter. FEBS Lett 2003;551:78–86. [PubMed: 12965208]
54. Guidotti A, Forchetti CM, Corda MG, Konkel D, et al. Isolation, characterization, and purification to homogeneity of an endogenous polypeptide with agonistic action on benzodiazepine receptors. Proc Natl Acad Sci USA 1983;80:3531–3535. [PubMed: 6304714]
55. Hengst U, Albrecht H, Hess D, Monard D. The phosphatidylethanolamine-binding protein is the prototype of a novel family of serine protease inhibitors. J Biol Chem 2001;276:535–540. [PubMed: 11034991]
56. Kinseth MA, Anjard C, Fuller D, Guizzunti G, et al. The Golgi-associated protein GRASP is required for unconventional protein secretion during development. Cell 2007;130:524–534. [PubMed: 17655921]
57. Nishino J, Yamashita K, Hashiguchi H, Fujii H, et al. Meteorin: a secreted protein that regulates glial cell differentiation and promotes axonal extension. EMBO J 2004;23:1998–2008. [PubMed: 15085178]

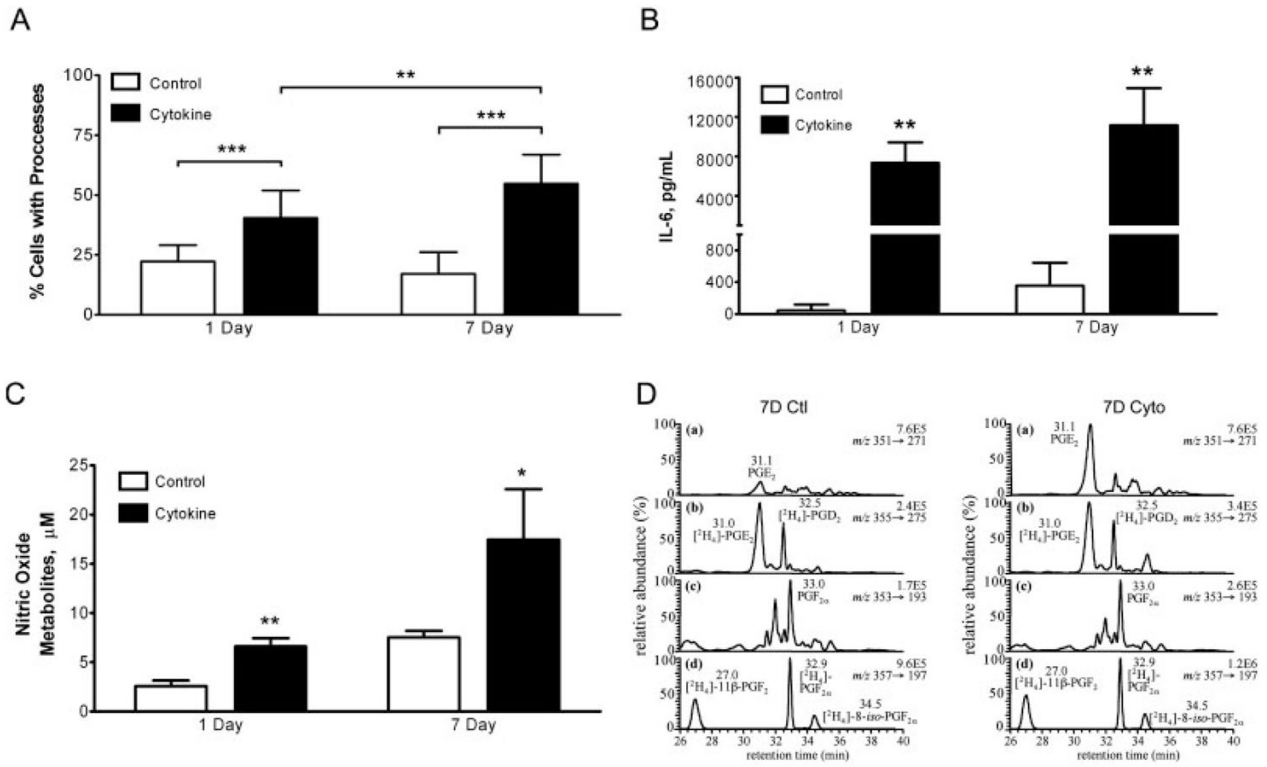

Figure 1.

Morphological and biochemical responses of murine astrocytes to cytokine exposure. (A) Quantification of percent GFAP-positive cells with processes. The percent of cells with processes were calculated from 3–6 fields/condition taken from three independent experiments. $^{**}p<0.01$, $^{***}p<0.001$ by unpaired, two-tailed *t*-test. (B) IL-6 production measured by ELISA in ACM. Data are reported as the mean±SD. $^{**}p<0.01$ by unpaired, two-tailed *t*-test (n = 3–6). (C) Nitric oxide synthase (NOS) activity measured by nitric oxide metabolite accumulation in ACM. Metabolites were measured by reductive chemistries coupled to chemiluminescence. Data are reported as the mean±SD. $^{*}p<0.05$, $^{**}p<0.01$ by unpaired, two-tailed *t*-test (n = 3–6). (D) LC-electron capture APCI/MRM/MS analysis of PGE_2 (a) and $PGF_{2\alpha}$ (c) in ACM from 7 days control-treated (left) and 7 days cytokine-treated (right) astrocytes. Concentrations of PGE_2 (retention time (rt) = 31.0 min) and $PGF_{2\alpha}$(rt = 33.0 min) were calculated by interpolation of linear regression curves constructed from authentic lipid standards. Variation due to sample processing and MS analysis was accounted for by addition of $[^2H_4]$-PGE_2 (b) and $[^2H_4]$-$PGF_{2\alpha}$ (d) internal standards.

A

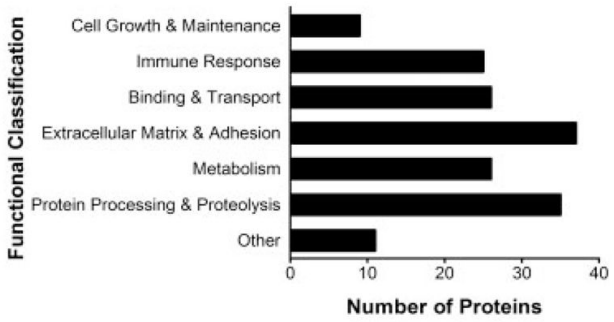

B

Interpro #	Description	Protein	Function
IPR006209	EGF-like	14	ECM & Adhesion
IPR008160	Collagen triple helix repeat	9	ECM & Adhesion
IPR012680	Laminin G, subdomain 2	9	ECM & Adhesion
IPR013151	Immunoglobulin	9	Immune
IPR013091	EGF calcium-binding	8	ECM & Adhesion
IPR012679	Laminin G, subdomain 1	7	ECM & Adhesion
IPR002049	EGF-like, laminin	6	ECM & Adhesion
IPR013162	CD80-like, immunoglobulin C2-set	6	Immune
IPR003961	Fibronectin, type III	6	ECM & Adhesion
IPR002035	von Willebrand factor, type A	5	ECM & Adhesion

C

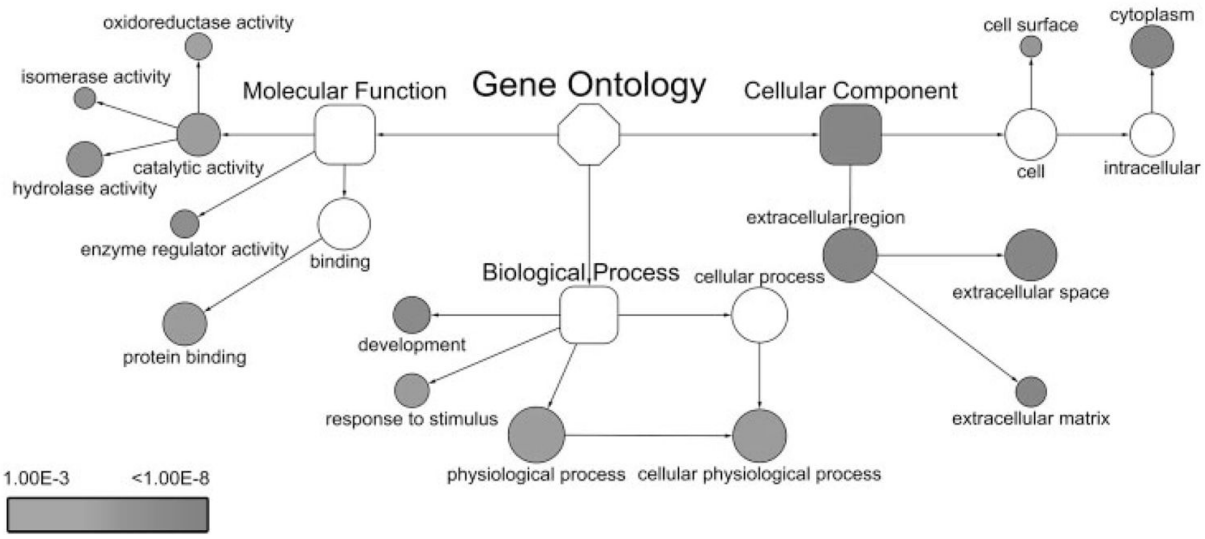

Figure 2.

Functional GO analysis of the astrocyte protein secretome. (A) Astrocyte protein secretome containing 169 proteins classified into broad functional categories. (B) InterPro domains (Top 10) represented by the astrocyte protein secretome. (C) Over-represented GO terms of the astrocyte protein secretome. Network visualization and statistical analysis was performed using BiNGO 2.0 implemented in the Cytoscape platform. Over-representation was determined for each GO term individually by comparing the proportion of genes assigned to each term from the astrocyte secretome to the proportion of genes assigned to that same term from the annotated mouse genome. Statistically significant over-representation was calculated by hypergeometric analysis and Benjamini & Hochberg false discovery rate (FDR) correction ($p<0.001$). Key represents range of *p*-values for significantly over-represented GO terms. To maintain hierarchical accuracy, parental GO terms that were not significantly over-represented are illustrated (white shapes). Relative sizes of shapes correspond to the number of members within that term.

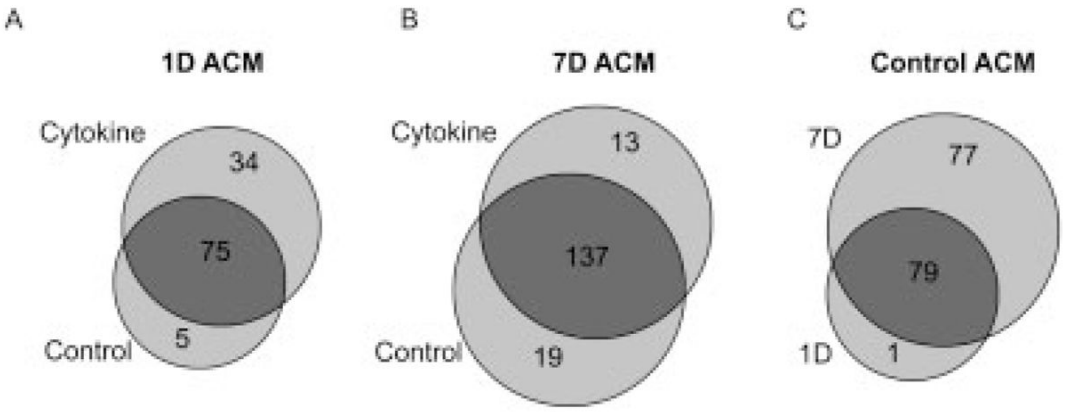

Figure 3.
Basal and cytokine-induced protein identifications in the astrocyte protein secretome. (A) Comparison of 1 day ACM between control and cytokine-treated astrocytes. (B) Comparison of 7 days ACM between control and cytokine-treated astrocytes. (C) Evaluation of control ACM between 1 day and 7 days cultured astrocytes.

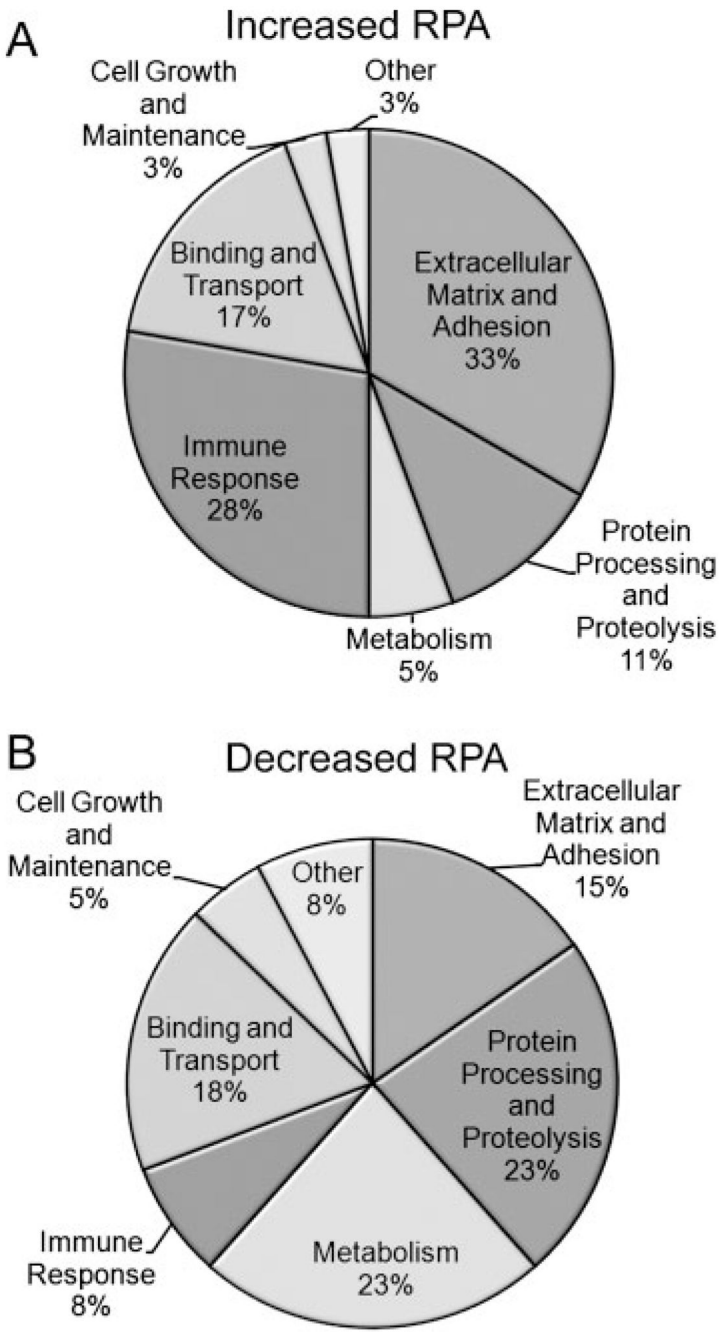

Figure 4.

Functional comparison of proteins with RPA changes after 7 days cytokine treatment. (A) Functional classification of proteins with increased RPA. Thirty-six proteins were classified, composed of 23 proteins with ≥2.5-fold increase in redundant peptides and 13 proteins that were unique to 7 days cytokine ACM. (B) Functional classification of proteins with decreased RPA. A total of 40 proteins were classified, composed of 21 proteins with ≥2.5-fold decrease in redundant peptides and 19 proteins that were unique to 7 days control ACM.

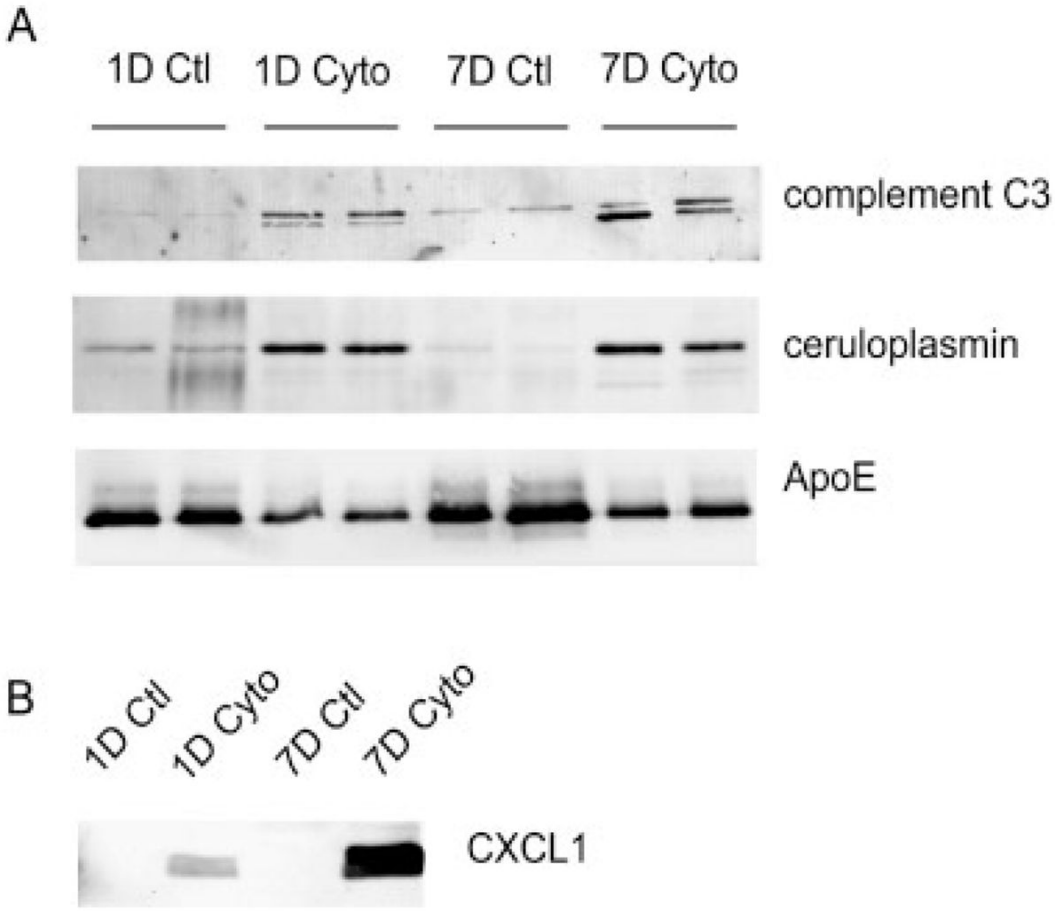

Figure 5.
Western blot validation of Gel/LC-MS/MS analysis. (A) Western blots for proteins predicted to have increased (complement C3, ceruloplasmin) or decreased (ApoE) RPA based on spectral count analysis. For each treatment condition, equal volumes of biological duplicates were loaded, corresponding to the identical conditions under which the MS analysis was performed. (B) Western blot for chemokine ligand 1 (CXCL1) showed detection only after cytokine stimulation. Equal protein (25 μg) was loaded per lane.

Table 1

Basal and cytokine-induced astrocyte secretome

Protein name (Synonym)	Accession[a)]	MW (kDa)	1 day control	1 day cytokine	7 days control	7 days cytokine
			Unique peptides[b)]			
Extracellular Matrix and Adhesion						
Agrin	A2ASQ0	205.0	6	26	8	27
Basement membrane-specific heparan sulfate proteoglycan core protein	Q05793	398.3	3	18	17	46
Cadherin-2 precursor (Neural-cadherin)	P15116	99.8	7	6	11	11
Calsyntenin 1	Q9EPL2	108.9	7	6	10	6
Collagen alpha-1(I) chain precursor	P11087	138.0	3	5	9	6
Collagen alpha-1(IV) chain precursor	P02463	160.7	-	-	2	3
c) Collagen alpha-1(VI) chain precursor	Q04857	108.5	-	2	-	3
d) Collagen alpha-1(XI) chain precursor	Q61245	181.0	-	-	2	-
Collagen alpha-1(XII) chain precursor	Q60847	340.2	3	13	41	27
Collagen alpha-2(I) chain precursor	Q01149	129.6	-	2	6	4
Collagen alpha-2(V) chain precursor	Q3U962	145.0	4	12	9	7
EGF-containing fibulin-like extracellular matrix protein 2	Q9WVJ9	49.4	3	4	11	4
Extracellular matrix protein	Q61508	62.8	-	-	7	4
Fat 1 cadherin	Q9QXA3	506.0	-	-	8	4
Fibromodulin precursor (FM)	P50608	43.1	4	5	6	6
Fibronectin 1	Q3UGY5	262.8	54	59	65	65
Fibulin-5 precursor (FIBL-5)	Q9WVH9	50.2	4	2	8	3
Galectin-3 (Galactose-specific lectin 3)	P16110	27.5	-	2	3	2
Glypican-4 precursor (K-glypican)	P51655	62.6	-	3	6	6
c) Intercellular adhesion molecule (Icam1)	Q922B3	58.9	-	-	-	4
c) Laminin subU alpha-4 precursor	P97927	201.8	-	-	-	7
Laminin subunit alpha-5 precursor	Q61001	404.0	-	7	2	23
c) Laminin subunit beta-2 precursor (S-laminin)	Q61292	196.4	-	8	-	19
Laminin subunit gamma-1 precursor (Laminin B2 chain)	P02468	177.3	-	11	4	25
Legumain	A2RTI3	49.4	2	6	6	6
Lysyl oxidase-like 3	Q91VN8	83.7	-	-	3	2

Protein name (Synonym)	Accession[a)]	MW (kDa)	1 day control	1 day cytokine	7 days control	7 days cytokine
			Unique peptides[b)]			
Mammalian ependymin related protein-2	Q99M71	25.5	7	7	8	7
Mimecan precursor (Osteoglycin)	Q62000	34.0	-	4	6	3
Mini-agrin	Q5EBX5	103.4	2	2	2	3
Neurocan core protein precursor (Chondroitin sulfate proteoglycan 3)	P55066	137.2	7	8	6	5
Nidogen 2 protein	Q8R5G0	153.9	3	-	7	2
SPARC-like protein 1 precursor (Matrix glycoprotein Sc1)	P70663	72.3	-	4	6	5
Tenascin precursor (TN-C)	Q80YX1	231.8	3	14	7	24
Tenascin-N precursor (TN-N)	Q80Z71	173.1	-	-	5	14
Thrombospondin 1	P35441	129.7	-	2	5	14
Vascular cell adhesion protein 1 precursor (CD106 antigen)	P29533	81.3	5	4	13	19
Vitamin K-dependent protein S precursor	Q08761	74.9	-	-	4	5
Protein Processing and Proteolysis						
78 kDa glucose-regulated protein precursor	P20029	72.4	8	8	9	5
α-2-macroglobulin-P precursor (α-2-macroglobulin)	Q6GQT1	164.3	38	48	51	47
Bone morphogenetic protein 1	P98063	111.7	2	4	3	4
Calreticulin precursor	P14211	48.0	3	2	3	-
Carboxypeptidase E precursor	Q00493	53.3	11	10	14	14
Cathepsin B precursor	P10605	37.3	13	11	13	13
Cathepsin D precursor	P18242	45.0	7	8	13	12
Cathepsin L1 precursor	P06797	37.5	7	3	7	7
Cathepsin S precursor	O70370	38.4	-	-	7	6
Cathepsin Z precursor	Q9WUU7	34.0	4	2	6	8
Cystatin-C precursor (Cystatin-3)	P21460	15.5	9	10	9	12
Dipeptidyl-peptidase 1 precursor (Cathepsin C)	P97821	52.4	-	2	2	3
Dipeptidyl-peptidase 2 precursor	Q9ET22	56.3	2	3	-	2
[d)] ER protein ERp29 precursor	P57759	28.8	-	-	3	-
Endoplasmin precursor (GRP94)	P08113	92.5	2	2	3	2
Glia-derived nexin precursor (Serpine 2)	Q07235	44.2	-	8	9	9
[d)] Inter-alpha-trypsin inhibitor heavy chain H3	Q61704	99.0	-	-	7	-

Proteomics. Author manuscript; available in PMC 2009 April 12.

Protein name (Synonym)	Accession[a)]	MW (kDa)	1 day control	1 day cytokine	7 days control	7 days cytokine
			Unique peptides[b)]			
Inter-alpha-trypsin inhibitor heavy chain H5	Q8BJD1	106.7	-	-	3	6
Lysosomal protective protein precursor	P16675	53.8	-	6	7	9
Metalloproteinase inhibitor 2 precursor (TIMP-2)	P25785	24.3	4	5	8	7
Peptidyl-prolyl cis-trans isomerase A	P17742	18.0	4	3	7	6
Peptidyl-prolyl cis-trans isomerase B	P24369	22.7	5	6	7	4
Plasma glutamate carboxypeptidase precursor	Q9WVJ3	51.8	6	6	7	5
Plasma protease C1 inhibitor	P97290	55.6	2	3	12	14
Plasminogen activator inhibitor 1	P22777	45.0	-	7	3	9
Pigment epithelium-derived factor (PEDF)	P97298	46.2	13	14	15	13
Protein disulfide-isomerase A3 precursor	P27773	56.7	10	11	13	6
Protein disulfide-isomerase A4 precursor	P08003	72.0	-	3	7	2
[d)] Protein disulfide-isomerase A6 precursor	Q922R8	48.1	-	-	3	-
Protein disulfide-isomerase precursor (PDI)	P09103	57.1	3	3	5	-
Puromycin-sensitive aminopeptidase	Q11011	103.3	2	6	3	-
Serine protease inhibitor A3N precursor (Serpin A3N)	Q91WP6	46.7	5	11	11	10
[c)] Stromelysin-1 precursor (MMP-3)	P28862	53.8	-	3	-	8
Sulfhydryl oxidase 1 precursor (Quiescin Q6)	Q8BND5	82.8	-	-	9	5
Tripeptidyl-peptidase 1 precursor	O89023	61.3	-	-	2	4
Metabolism						
Acid ceramidase precursor (Acylsphingosine deacylase)	Q9WV54	44.7	-	-	4	5
α-N-acetylglucosaminidase	O88325	82.6	-	-	3	3
Aspartate aminotransferase	P05202	47.4	3	4	4	2
[d)]β-1,3-N-acetylglucosaminyltransferase lunatic fringe	O09010	42.0	-	-	3	-
[d)]β-glucuronidase precursor	P12265	74.2	-	-	5	-
β-hexosaminidase alpha chain precursor (Hexosaminidase A)	P29416	60.6	-	-	4	2
β-hexosaminidase beta chain precursor (Hexosaminidase B)	P20060	61.1	4	3	13	4
[d)] Bifunctional heparan sulfate N-deacetylase/N-sulfotransferase 1	Q3UHN9	100.7	-	-	3	-
Chitinase-3-like protein 1 precursor (Cartilage glycoprotein 39)	Q61362	43.0	5	16	14	15
Epididymis-specific alpha-mannosidase precursor	O54782	115.6	2	10	7	6

Protein name (Synonym)	Accession[a)]	MW (kDa)	1 day control	1 day cytokine	7 days control	7 days cytokine
			Unique peptides[b)]			
Exostosin-2	P70428	82.1	-	-	5	2
Galactocerebrosidase precursor (GALCERase)	P54818	75.5	-	-	3	2
Gamma-glutamyl hydrolase precursor	Q9Z0L8	35.4	2	2	5	4
Ganglioside GM2 activator precursor	Q60648	20.8	3	3	3	2
Glucose-6-phosphate isomerase (GPI)	P06745	62.8	7	5	7	4
[c)] Lysosomal alpha-glucosidase precursor (Acid maltase)	P70699	106.2	-	-	-	4
N-acetylglucosamine-6-sulfatase precursor (G6S)	Q8BFR4	61.2	-	3	4	4
[d)] N-acetyllactosaminide beta-1,3-N-acetyl-glucosaminyltransferase	Q8BWP8	47.4	-	-	4	-
N(4)-(beta-N-acetylglucosaminyl)-L-asparaginase precursor	Q64191	37.0	-	3	3	4
Palmitoyl-protein thioesterase 1 precursor (PPT-1)	O88531	34.5	-	-	5	5
Platelet-activating factor acetylhydrolase	Q60963	49.2	-	2	8	2
Procollagen-lysine, 2-oxoglutarate 5-dioxygenase 1 (Lysyl hydroxylase 1)	Q9R0E2	83.6	3	4	14	7
Procollagen-lysine, 2-oxoglutarate 5-dioxygenase 2 (Lysyl hydroxylase 2)	Q9R0B9	84.5	-	3	5	3
Procollagen-lysine, 2-oxoglutarate 5-dioxygenase 3 (Lysyl hydroxylase 3)	Q9R0E1	84.9	-	-	7	6
Putative phospholipase B-like 2 precursor	Q3TCN2	66.7	-	2	2	5
Ribonuclease T2 isoform 1	Q9CQ01	29.6	2	-	3	5
Immune						
β-2-microglobulin precursor	P01887	13.8	2	2	3	5
[d)] Cell adhesion molecule four precursor	Q8R464	42.7	-	-	4	-
[c)] Chemokine (C-C motif) ligand 7	Q03366	11.0	-	-	-	3
[c)] Chemokine (C-C motif) ligand 8	Q9Z121	11.0	-	-	-	3
[c)] Chemokine (C-X3-C motif) ligand 1 (Fractalkine)	O35188	42.1	-	-	-	4
[c)] Chemokine (C-X-C motif) ligand 1 (Growth-regulated alpha protein)	P12850	10.3	-	3	-	3
Complement C1q subcomponent subunit B precursor	P14106	26.7	-	-	2	3
Complement C1q tumor necrosis factor-related protein 5 precursor	Q8K479	25.4	3	5	3	4
Complement C3 precursor	P01027	186.5	33	72	66	89

Protein name (Synonym)	Accession[a)]	MW (kDa)	1 day control	1 day cytokine	7 days control	7 days cytokine
			Unique peptides[b)]			
Complement C4-B precursor	P01029	192.9	12	7	40	39
Complement C1q subcomponent subunit C precursor	Q02105	26.0	-	-	3	3
Complement C1r-A subcomponent	Q8CG16	80.1	-	4	9	15
Complement C1s-A subcomponent	Q8CG14	77.4	-	-	7	19
Complement factor B precursor	P04186	85.0	-	-	4	18
Cyclophilin C-associated protein	O35649	64.1	4	-	8	12
H-2 class I histocompatibility antigen, D-B alpha chain precursor	P01899	40.8	-	2	4	4
H-2 class I histocompatibility antigen, Q8 alpha chain	P14430	37.5	-	5	3	4
Ig superfamily containing leucine-rich repeat	Q6GU68	45.6	2	4	3	2
Lysozyme C type M precursor	P08905	16.7	-	-	4	3
Macrophage colony-stimulating factor 1 precursor (CSF-1)	P07141	60.6	2	5	4	8
d) Macrophage colony-stimulating factor 1 receptor	P09581	109.3	-	-	3	-
Macrophage migration inhibitory factor (MIF)	P34884	12.5	3	2	2	3
Monocyte differentiation antigen CD14 precursor	P10810	39.2	-	2	9	6
Pentraxin-related protein PTX3 precursor	P48759	41.8	5	10	3	11
Platelet-derived growth factor receptor-like protein precursor	Q6PE55	41.9	-	2	2	3
Binding and Transport						
45 kDa calcium-binding protein precursor (SDF-4)	Q61112	42.1	2	2	4	5
d) Acyl-CoA-binding protein (ACBP)	P31786	10.0	-	-	3	-
c) Adipocyte enhancer-binding protein	Q640N1	128.4	-	-	-	6
Annexin A2	P07356	38.7	6	2	8	-
Apolipoprotein E precursor (Apo-E)	P08226	35.9	10	3	14	13
d) Biotinidase precursor	Q8CIF4	58.6	-	-	3	-
Ceruloplasmin	Q61147	121.2	12	34	24	47
Dystroglycan precursor (Dystrophin-associated glycoprotein 1)	Q62165	96.9	5	4	10	7
Follistatin-related protein 1 precursor	Q62356	34.6	5	9	7	12
Gelsolin precursor (Actin-depolymerizing factor)	P13020	85.9	2	-	8	3
Lipopolysaccharide binding protein	Q61805	53.1	-	5	5	6
c) Lysosomal-associated membrane glycoprotein 1 (LAMP1)	P11438	43.9	-	-	-	3

Protein name (Synonym)	Accession[a)]	MW (kDa)	1 day control	1 day cytokine	7 days control	7 days cytokine
			Unique peptides[b)]			
Neutrophil gelatinase-associated lipocalin precursor (Lipocalin 2)	P11672	22.9	-	6	5	7
Nucleobindin-1 precursor (CALNUC)	Q02819	53.4	2	9	7	7
Phosphatidylethanolamine-binding protein 1 (PEBP-1)	P70296	20.8	4	5	6	4
Phospholipid transfer protein precursor (Lipid transfer protein II)	P55065	54.5	3	-	16	13
Rab GDP dissociation inhibitor beta	Q61598	50.5	4	5	9	3
Renin receptor precursor	Q9CYN9	39.1	-	-	2	3
SPARC precursor	P07214	34.3	11	11	12	11
Serotransferrin precursor (Transferrin)	Q921I1	76.7	-	-	12	3
[d)] Sortilin-related receptor, LDLR class A repeats- containing	O88307	247.1	-	-	3	-
Sulfated glycoprotein 1 precursor (Prosaposin)	Q61207	61.4	2	4	12	13
Superoxide dismutase, extracellular	O09164	27.4	-	-	5	6
Transcobalamin-2 precursor	O88968	47.6	7	7	8	9
Vacuolar ATP synthase subunit S1 precursor	Q9R1Q9	51.0	-	4	5	5
Vesicular integral-membrane protein VIP36 precursor	Q9DBH5	40.4	-	-	3	4
Cell Growth & Maintenance						
Epididymal secretory protein E1 precursor	Q9Z0J0	16.4	4	5	5	5
Growth-arrest-specific protein 6 precursor (GAS-6)	Q61592	74.6	-	-	6	4
Insulin-like growth factor-binding protein 2	P47877	32.8	8	4	13	13
Insulin-like growth factor-binding protein 3	P47878	31.7	-	2	3	3
Insulin-like growth factor-binding protein 5	Q07079	30.4	3	4	4	6
Insulin-like growth factor-binding protein 7	Q61581	28.9	-	2	5	12
[d)] Plexin domain-containing protein 2 precursor	Q9DC11	59.6	-	-	3	-
Prolow-density lipoprotein receptor-related protein 1 precursor (A2MR)	Q91ZX7	504.7	-	-	4	5
Ptprz1 protein (DSD-1 Proteoglycan)	B2RXS8	164.4	3	3	6	5
Other						
4632419I22Rik protein	Q6NXM5	31.9	-	-	4	3
Acid sphingomyelinase-like phosphodiesterase 3a precursor	P70158	49.9	-	-	3	2
Amyloid beta A4 protein precursor (APP)	P12023	86.7	2	5	8	8
CD109 antigen precursor	Q8R422	161.7	-	5	10	3

Protein name (Synonym)	Accession[a)]	MW (kDa)	1 day control	1 day cytokine	7 days control	7 days cytokine
			Unique peptides[b)]			
Clusterin precursor (Apolipoprotein J)	Q06890	51.7	10	4	15	18
[d)] Meteorin-like protein	Q8VE43	34.5	-	-	3	-
Profilin 1	P62962	11.8	6	6	6	5
Retinoic acid receptor responder protein 2 precursor	Q9DD06	18.4	-	-	3	4
Secretogranin 3	P47867	53.3	2	2	14	4
Thioredoxin-dependent peroxide reductase	P20108	28.1	-	-	2	3
Vimentin	P20152	53.7	18	20	23	20

Proteins are organized by functional category and reported with their corresponding Uniprot accession number, molecular weight (MW), and unique peptides identified for each treatment condition.

[a)] Accession numbers are reported from the Uniprot database (www.uniprot.org) and, when available, refer to the unprocessed precursor protein.

[b)] The average numbers of unique peptides identified are reported for protein identifications that passed the selection criteria as detailed in the Experimental Procedures. A null value indicates the protein did not meet the minimum criteria for identification.

[c)] Protein was exclusively detected under cytokine-treated conditions.

[d)] Protein was exclusively detected under control conditions.